VOL. 46 | **SPECIAL ISSUE SI TEC 2023 2025** | PP 1-20



dx.doi.org/10.17488/RMIB.46.SI-TAIH.1514

E-LOCATION ID: e1514

# Optimizing Electrode Performance in EMG and EIT for Superior Muscle Data Acquisition

## Optimización del Rendimiento de los Electrodos en EMG y EIT para una Mejor Adquisición de Datos Musculares

Irán Arane Melchor Uceda¹© ◙, José Antonio Gutiérrez Gnecchi ¹©, Alberto González Vázquez²©, Enrique Reyes Archundia ¹©, Juan Carlos Olivares Rojas¹©, Arturo Méndez Patiño¹©, Alejandro Israel Robledo Ayala¹©

<sup>1</sup>Instituto Tecnológico de Morelia - División de Estudios de Posgrado e Investigación/ Tecnológico Nacional de México - México <sup>2</sup>Auckland University of Technology - School of Engineering, Computer and Mathematical Sciences - New Zealand

#### **ABSTRACT**

Optimizing electrode performance in electromyography (EMG) and electrical impedance tomography (EIT) is critical to advancing muscle data acquisition. This study systematically evaluates various electrode types, shapes, and materials, focusing on optimizing signal-to-noise ratio, durability, and long-term usability. A key contribution of this research is the identification of stainless-steel electrodes as the most efficient option, demonstrating superior signal stability, oxidation resistance, and reusability compared to disposable alternatives. This finding not only improves the reliability of EMG and EIT measurements but also offers a sustainable and cost-effective solution for clinical and research applications. By providing empirical evidence on electrode selection and design, this study lays the foundation for improved methodologies in rehabilitation, sports medicine, and neurology, ultimately improving patient care and deepening understanding of muscle physiology.

KEYWORDS: EMG, EIT, electrodes, isometric contraction, isotonic contraction.

#### **RESUMEN**

Optimizar el rendimiento de los electrodos en la electromiografía (EMG) y la tomografía de impedancia eléctrica (EIT) es fundamental para avanzar en la adquisición de datos musculares. Este estudio evalúa sistemáticamente varios tipos, formas y materiales de electrodos, centrándose en optimizar la relación señal/ruido, la durabilidad y la usabilidad a largo plazo. Una contribución clave de esta investigación es la identificación de los electrodos de acero inoxidable como la opción más eficiente, demostrando una estabilidad de señal superior, resistencia a la oxidación y reutilización en comparación con las alternativas desechables. Este hallazgo no solo mejora la confiabilidad de las mediciones de EMG y EIT, sino que también ofrece una solución sostenible y rentable para aplicaciones clínicas y de investigación. Al proporcionar evidencia empírica sobre la selección y el diseño de electrodos, este estudio sienta las bases para mejorar las metodologías en rehabilitación, medicina deportiva y neurología, lo que en última instancia mejora la atención al paciente y profundiza la comprensión de la fisiología muscular.

PALABRAS CLAVE: Contracción isométrica, contracción isotónica, electrodos, EMG, EIT

## **Corresponding author**

TO: IRÁN ARANE MELCHOR UCEDA

INSTITUTION: INSTITUTO TECNOLÓGICO DE MORELIA - DIVISIÓN
DE ESTUDIOS DE POSGRADO E INVESTIGACIÓN/ TECNOLÓGICO

NACIONAL DE MÉXICO, MICHOACÁN- MÉXICO

ADDRESS: AVENIDA TECNOLÓGICO 1500, MORELIA,

MICHOACÁN, C.P. 58120, MÉXICO. EMAIL: iran.mu@morelia.tecnm.mx **Received:** 

30 January 2025

Accepted:

14 April 2025

**Published:** 

#### INTRODUCTION

Electromyography (EMG) and electrical impedance tomography (EIT) have been established as key tools in the assessment of muscle activity and changes in the electrical properties of tissues.

EMG is considered a non-invasive technique<sup>[1]</sup>, capable of detecting, recording and interpreting electrical activities produced by the generation of action potentials in muscle fibers<sup>[2]</sup>, where their amplitudes are in the range of 0 to 5 mV, and their energy is concentrated in the range of 10 to 500 Hz<sup>[3]</sup> (see Figure 1). Surface electromyography (sEMG) signals contain information widely applied in prosthetics<sup>[4]</sup>, rehabilitation<sup>[5]</sup>, collaboration between humans and robots<sup>[6]</sup> and teleoperation<sup>[7]</sup>. However, one of the main challenges that must be overcome in real-life environments are electrode displacement<sup>[8][9]</sup>, arm position changes<sup>[10][11]</sup>, fatigue<sup>[12]</sup>, and time-related effects<sup>[13]</sup>.

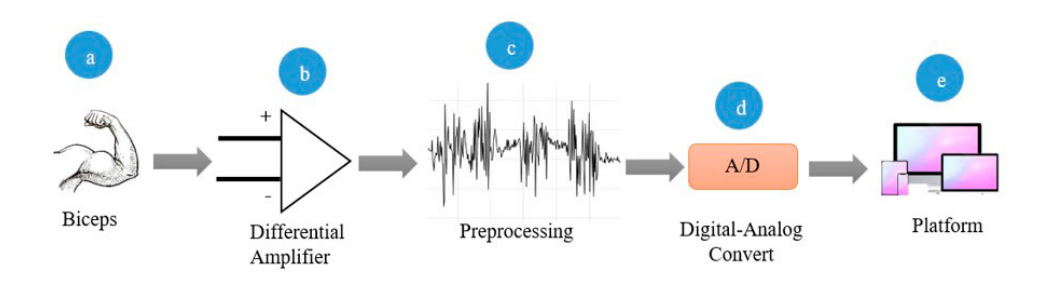


FIGURE 1. Surface electromyography block diagram. a) Detection of biceps myoelectric potentials. b) Biopotential amplification. c) Signal filtering and conditioning. d) A/D conversion. e) Data visualization.

Complementary and novel techniques are entering the world of biopotentials, driven by the need to extract and analyze the vast amount of information they contain, which often cannot be captured efficiently with conventional methods. A prominent example is electrical impedance tomography (EIT), a noninvasive bioelectrical potential technique<sup>[14]</sup> that uses small electrical currents to measure changes in tissue impedance, allowing for real-time image reconstruction (see Figure 2). EIT is not only safe and radiation-free, but also offers advantages such as portability and reduced costs compared to other imaging modalities. This makes it especially useful for clinical applications such as electromyometrial imaging (EMMI), predicting premature delivery<sup>[15]</sup>, pulmonary vein isolation imaging<sup>[16]</sup>, or characterizing myocardial infarction through EEG signals<sup>[17]</sup>.

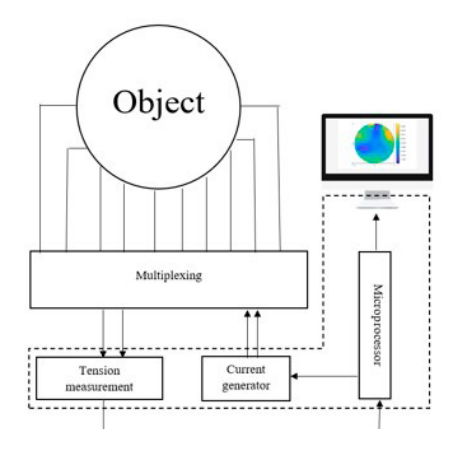


FIGURE 2. Block diagram of an EIT system.

The aim of this research is to evaluate the potential of combining EMG and EIT to optimize the assessment of muscle function in rehabilitation, integrating the information obtained from both techniques to more accurately understand muscle changes and develop personalized treatments. The quality of the signals obtained by EMG and EIT is directly influenced by the selection of the electrodes, whose materials and geometries have a significant impact on the signal-to-noise ratio and the accuracy of the measurements<sup>[18][19]</sup>. Although disposable silver/silver chloride (Ag/AgCl) electrodes are widely used due to their excellent performance, their high cost and the environmental impact associated with their use represent important limitations, especially in resource-limited settings. Therefore, this study focuses on evaluating the performance of reusable electrodes made of materials such as stainless steel and nickel-copper alloy, comparing key metrics such as signal-to-noise ratio and root mean square error. The expected results include the identification of electrode materials and designs that offer the lowest error and highest efficiency compared to Ag/AgCl electrodes, laying the foundation for their application in EMG and EIT in a sustainable and accessible way.

#### Literature review

The integration of techniques such as electromyography (EMG) and electrical impedance tomography (EIT) has been a central focus in recent studies due to their ability to offer complementary assessments of muscle activity. Morgado (2021) initiated the foundations of the study of bioelectricity by demonstrating the ability of living organisms to generate electricity through experiments with isolated nerves and muscles, paving the way for subsequent research on electrical behavior in biological tissues<sup>[20]</sup>. Barrios et al. (2020) contributed to this field by analyzing electrical conductivity in different tissues and materials through the use of metallic electrodes, showing variations in conductivity depending on the material used and highlighting the need to control physiological variables to improve precision in applications such as electrotherapy<sup>[21]</sup>. In this context,<sup>[12]</sup>, further investigated the sensitivity of EIM during voluntary muscle contractions of the biceps brachii, observing a significant decrease in impedance during muscle contraction and expanding the knowledge on the usefulness of this technique to assess muscle dynamics<sup>[22]</sup>. Starting in 2020, myoelectric signals began to have a greater impact on the control of robotic arms, through the development of a control system based on SVM models, based on the analysis and classification of sEMG signal patterns from the hand, marking significant advances in brain-machine interfaces, although with limited application to specific hand movements<sup>[23]</sup>. Wang et al. (2020) investigated the relationship between electrical impedance and muscle fatigue using statistical models and tests at different measurement angles of the biceps, identifying the influence of external factors such as temperature and hydration, underlining the importance of standardizing experimental conditions to obtain reliable measurements<sup>[24]</sup>. Furthermore, Freeborn et al. (2020) studied how physical activity affects muscle impedance, revealing that essentially active individuals present a lower impedance compared to sedentary ones, which, although limited to a small sample, provides evidence on the relationship between bioimpedance and physical activity<sup>[25]</sup>. In a related study, Freeborn and Fu (2018) analyzed the accuracy of bioimpedance measurements in biceps tissues during exhausting exercises, contributing to improve the accuracy of bioimpedance measurement equipment through the analysis of relative errors in resistance<sup>[26]</sup>. Finally, Rutkove and Sánchez (2019) explored EIM as a tool for monitoring neuromuscular diseases, highlighting its sensitivity to track the progression of pathologies through varied exercise protocols, although they pointed out the need to improve calibration and minimize the influence of external factors<sup>[27]</sup>.

Taken together, the work carried out in this field reinforces the feasibility of combining EMG and EIT for the assessment of muscle and other pathologies (Figure 3). Recent studies have shown that this conjunction is particularly useful in biceps muscle activation protocols, as observed in experiments where both techniques allow the assess-

ment of muscle progression in both sedentary and active individuals. The advances highlight the potential of integrating both tools into portable devices that can be applied in clinical, sports and rehabilitation contexts.

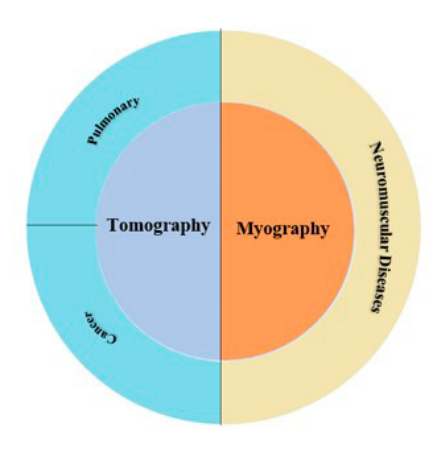


FIGURE 3. Diagnosis of the disease and clinical follow-up of EMG and EIT.

## Electromyography (EMG) and Electrical Impedance Tomography (EIT) Electromyography (EMG)

Electromyography (EMG) is a biomedical measurement tool used to assess muscle motor activity and localize peripheral lesions. Muscle electrical activity is the result of cell shortening, leading to general muscle contraction and generating a biopotential<sup>[28]</sup>. This activity stimulates several muscle groups<sup>[29]</sup>, joints<sup>[30]</sup>, upper and lower limbs<sup>[31]</sup>, as well as the spine (Farina *et al.*, 2003). Despite being a relatively simple measurement technique, quantifying EMG signals can be quite complicated<sup>[32]</sup>. Figure 4 illustrates muscle contraction as a response of muscle fibers to the all-or-none process.

According to<sup>[33]</sup>, the resting state is the inactive condition of a cell before and after generating an action potential. When a stimulus excites the cell with a current exceeding the threshold, an action potential is triggered; otherwise, the cell remains in a resting state, known as the failed state. During depolarization, the membrane potential changes from negative to positive, giving rise to the action potential. Repolarization then occurs, as the cell returns to its resting state by transitioning from a positive to a negative potential. Finally, the refractory period occurs, during which the cell is temporarily unable to respond to new stimuli, ensuring proper signal propagation.

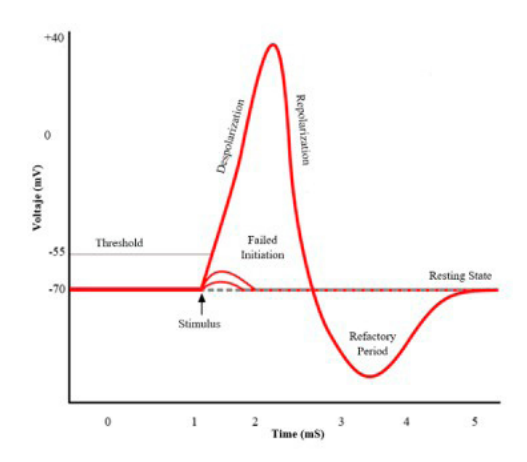


FIGURE 4. Action potential and its division.

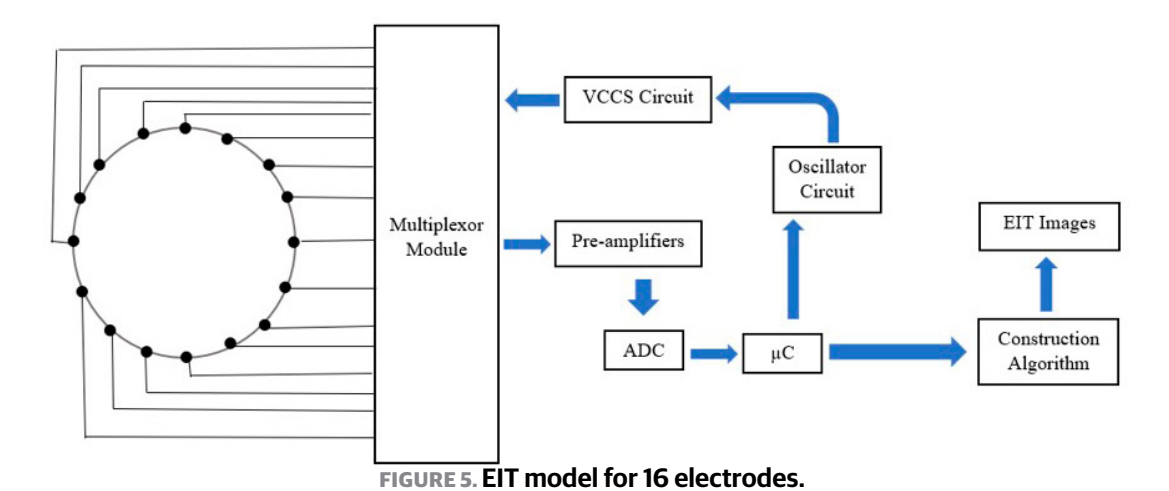
According to Lee *et al.*<sup>[34]</sup>, Table 1 provides a detailed overview of the amplitude and frequency variations of various biological signals that the human body can generate.

•		•
Signal Type	Frequency Range	Amplitude
Electroencephalogram	0.5-60Hz	15-100μV
Electromyogram	10-200Hz	0.1-5 μV
Electrocardiogram	0.05-250Hz	100 μV (child) 5mV (young)
Electrogastogram	0.7-70Hz	2mV
Electroneurogastogram	250-5000Hz	0-100 μV

TABLE 1. Frequency ranges for biomedical signals.

#### Electrical Impedance Tomography (EIT)

Electrical Impedance Tomography (EIT) is an advanced noninvasive medical imaging technique that allows the evaluation of the conductivity or permittivity distribution of the human body. This procedure is carried out by placing conductive electrodes on the surface of the skin, where low-intensity electrical currents are applied and the resulting electrical potentials are measured to obtain an image of the internal impedance of the body<sup>[35][36]</sup> (see Figure 5). EIT has proven useful in a variety of fields, being used in the quality control of materials, such as polymers or composite materials, where its ability to detect variations in conductivity is of great use<sup>[37]</sup>. In addition, the technique is used in geological exploration to identify variations in the electrical properties of the subsoil, which facilitates the detection of natural resources or the evaluation of geological conditions<sup>[38]</sup>. In the medical field, EIT is used to visualize and diagnose a wide range of conditions, including lung disorders, heart disease, nervous system problems and muscle pathologies<sup>[39]</sup>.



EIT operates in a range between 2 kHz and 200 kHz, allowing for higher spatial and temporal resolution when imaging internal body tissues<sup>[35]</sup>. Table 2 details different organs with frequencies determined according to<sup>[40]</sup>.

Due to these differences in frequency ranges, EMG and EIT signals offer valuable complements in the analysis of muscle function. In this regard, recent studies have shown that the combination of both techniques allows a more accurate assessment of muscle contractions, since EMG captures the electrical activity in the muscle while EIT allows visualizing changes in the distribution of internal impedance, providing a more complete view of muscle physiology<sup>[41][42][43]</sup>.

Tissue	Resistivity (MΩ)	Frequency (kHz)		
CsH	65	10		
Blood	135-161	10		
Muscle <sup>a</sup>				
Longitudinal	150	10		
Transverse	2300	10		
Bone a, b				
Longitudinal	5000	10		
Longitudinal	1000	1000		
Radial	16600	10		
Radial	5300	1000		
<sup>a</sup> The measurement of this organ is carried out in two planes				
<sup>b</sup> The measurement of this organ was carried out at two different frequencies				

TABLE 2. Resistivity values of different organs at given frequencies.

#### **Biceps injuries**

Biceps injuries encompass a variety of conditions affecting the biceps muscle and its tendons, which are usually the result of overuse, acute trauma, or degenerative changes, and are common in middle-aged men and usually affect the dominant arm. These injuries range from tendinosis and bursitis to partial or complete tears, with the diagnosis being confirmed through clinical history, physical examination, and imaging techniques such as ultrasound or MRI. Treatment varies depending on the severity, being conservative in cases of partial injuries or tendinosis, and surgical in complete tears, especially if the patient has high physical demands. Post-surgical rehabilitation is crucial to recover strength and joint range. In injuries to the long tendon of the biceps, treatment can also be conservative or surgical, with techniques such as tenotomy or tenodesis, which have shown good results in improving shoulder function.

#### MATERIALS AND METHODS

The proper performance of electrodes in EMG and EIT signal acquisition depends on multiple factors, including material composition, electrode geometry, and their interaction with the subject's skin. In this study, a controlled experimental protocol was developed to comparatively evaluate different types of electrodes in terms of signal quality, stability over long-term measurements, and resistance to oxidation.

To conduct this study, an experimental protocol illustrated in Figure 6 was implemented, detailing the experimental procedures, electrode layout, materials evaluated, and the techniques used in signal acquisition and data analysis.

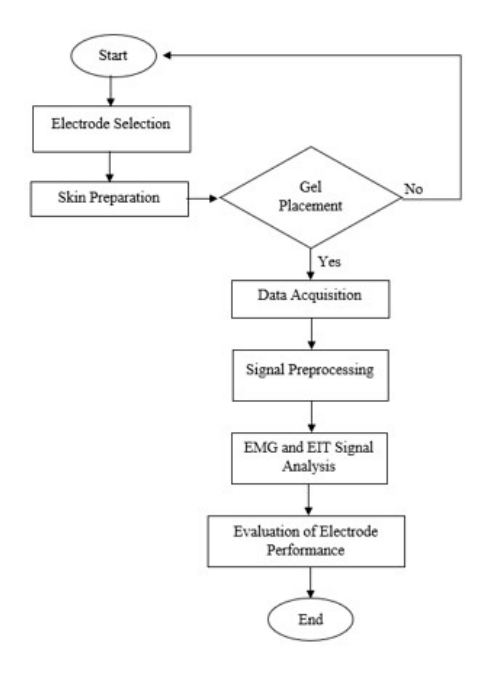


FIGURE 6. Signal acquisition.

#### Participants and experimental protocol

Five healthy male participants (aged 20–26 years) were recruited to conduct a controlled analysis of electrode performance, ensuring methodological feasibility and measurement consistency. Participants performed a structured routine consisting of five different biceps-targeting exercises, each with a repetition schedule of three sets of 20 repetitions, for a total of 13 sessions. The exercises were designed to progressively induce muscle fatigue, allowing electrode performance to be assessed under increasing physiological stress. Repetitions continued until muscle failure was reached, ensuring a thorough evaluation of signal stability at different levels of fatigue.

## Electrode placement for electromyography and electrical impedance tomography

During the experimental sessions, EMG and EIT electrode placement was performed on each subject (Figure 7) following standardized procedures. For EMG measurements, placement was carried out according to the SENIAM protocol<sup>[44]</sup>, ensuring precise anatomical placement over the biceps muscles. For EIT, an array of 16 adjacent electrodes was placed around the muscle region, ensuring a uniform and reproducible distribution across measurement sessions. In addition, to minimize variability in skin-electrode impedance and improve stability in data acquisition, participants' skin was prepared by meticulously cleaning the area and applying conductive gel before each session.

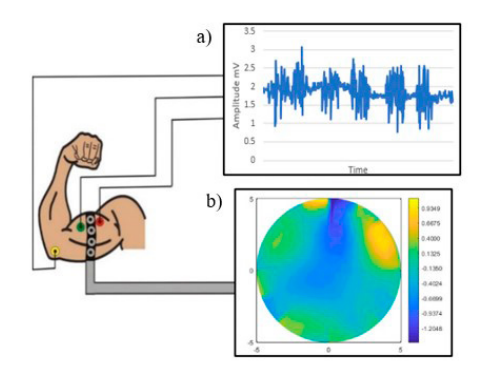


FIGURE 7. Placement of the electrodes. a) Placement by EMG. b) Placement by EIT.

#### Electrode set

To optimize EMG and EIT signal acquisition, a variety of electrodes with variations in material, shape, and size had to be manufactured and evaluated (Figure 8). Their performance was compared, considering key parameters such as signal-to-noise ratio, impedance stability, and durability over time, to identify the optimal configuration for capturing muscle signals. Furthermore, the electrodes were selected based on their conductivity, corrosion resistance, biocompatibility, ease of manufacture, cost, and accessibility, seeking a balance between efficiency and economic viability. Tests were also conducted to assess potential irritation or allergic reactions when in contact with the patient's skin. Finally, the sustainability of the materials was assessed, taking into account their reusability and environmental impact, allowing for the selection of more environmentally friendly options without compromising system efficiency.

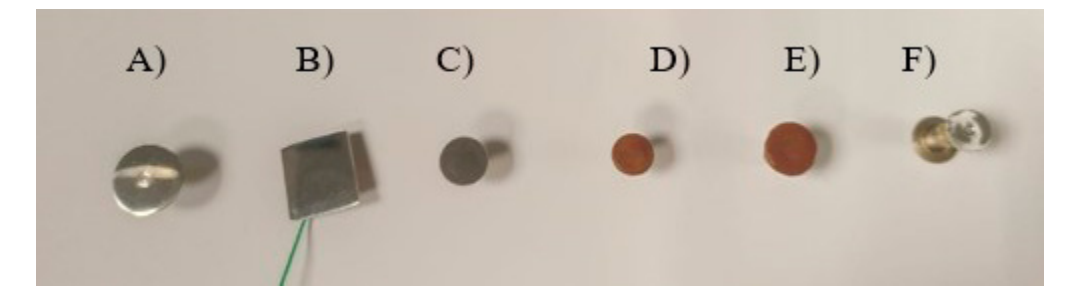


FIGURE 8. Assorted electrodes. A) Circular stainless-steel electrode (1 cm ∅). B) Square stainless-steel electrode. C) Circular electrode with a nickel alloy. D) Circular electrode (0.8 cm ∅) with a copper alloy. E) Circular electrode (1 cm ∅) with a copper alloy. F) Needle electrode.

Table 3 presents a comparative summary of the characteristics of the electrodes analyzed, detailing their manufacturing material, geometry, dimensions, reusability, and operating frequency range. This comparison is essential to determine which type of electrode offers the best conditions for EMG and EIT signal acquisition, thus improving the accuracy and reliability of measurements.

Electrode Material	Reusability	Frequency Range (Hz)	Performance in EMG	Performance in EIT
Circular stainless-steel electrode (1 cm Ø)	High	5-2500Hz	Good	Good
Square stainless-steel electrode	High	0.5-5000Hz	Best	Best
Circular electrode with a nickel alloy	Medium	10-1500Hz	Moderate	Moderate
Circular electrode (0.8 cm Ø) with a copper alloy	Low	20-1200Hz	Limited	Limited
Circular electrode (1 cm Ø) with a copper alloy	Low	15-1500Hz	Moderate	Moderate
Needle electrode	High	10-300Hz	High	NA

TABLE 3. Features and performance of EMG and EIT electrodes

#### **Data acquisition system**

For data acquisition, a system developed independently for EMG (Figure 9) and EIT (Figure 10) was implemented.

In each of these processes, various electrode materials were used to evaluate how their characteristics influenced the quality of the data obtained, allowing for a detailed comparison between the results of each configuration.

For EMG signal acquisition, a system composed of several interconnected modules was used. The electrodes were placed on the patient's biceps muscle, capturing the electrical activity generated by muscle contractions. To ensure accurate and interference-free measurements, an INA128 instrumentation amplifier was used, widely used in biomedical applications due to its high accuracy and low noise level. This amplifier has adjustable gain, which in this case was set to 11, allowing it to amplify the low-amplitude signals generated by muscle contractions without distorting them. The INA128 was interconnected with the ISO122PGA amplifier, an isolation amplifier designed to protect both the system and the patient from potential electric shocks, in addition to reducing noise caused by electromagnetic interference. To filter the EMG signals and eliminate noise outside the band of interest, a band-pass filter was applied with a frequency range between 20 and 500 Hz, allowing the capture of high-frequency muscle signals while eliminating unwanted components, such as low-frequency noise.

For the acquisition and processing of EIT data, proprietary software<sup>[36][45]</sup> was implemented, which employs an optimized virtual approach to improve the quality of measurements and facilitate its integration with different hardware platforms. The 104-sample reconstruction approach was designed to generate more detailed and higher-resolution images, improving diagnostic accuracy and real-time monitoring of rehabilitation processes.



FIGURE 9. Schematic diagram of the experimental setup for EMG.

For the acquisition of EIT data, a low-frequency alternating current, specifically 50 kHz, with a voltage of 1 mV was applied through electrodes placed on the surface of the participant's body. This current was introduced into the area of interest in order to generate an electric field that would allow information to be obtained on the conductive properties of the tissue. The potential difference between the pairs of electrodes placed at specific points on the body surface was then measured, providing data on the variations in electrical impedance as the current moved through the tissues. These voltage values were then used as input to a back-projection-based image reconstruction algorithm, which allowed detailed visual representations of the electrical impedance distribution in the analyzed region to be generated, providing an accurate view of how conductivity is distributed in the surrounding muscles and tissues.

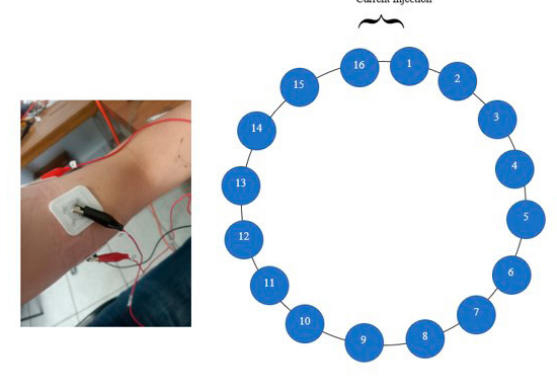


FIGURE 10. Schematic diagram of the experimental setup for EIT.

#### Data analysis

To evaluate electrode performance, several quantitative metrics were calculated, each of which provides relevant information about the quality of the acquired signals and the effectiveness of the electrodes used in the study.

## **Principal Component Analysis (PCA)**

It was used to reduce the dimensionality of EMG data and facilitate the identification of significant patterns in the signal. PCA is especially useful when there are a large number of variables (e.g., in EMG data) and the main sources of variation are to be identified.

PCA transforms the original data into a new coordinate system, where the first principal components explain most of the data variance. Its formula is denoted by Equation (1).

$$Z = X \cdot W \tag{1}$$

Where:

Z: Is the principal component matrix.

X: Is the centered data matrix (with zero mean).

W: is the eigenvector matrix (principal components).

#### **RESULTS AND DISCUSSION**

In this section, we present and discuss the results obtained from the evaluation of different types, shapes, and materials of EMG and EIT electrodes, taking into account various factors in order to optimize the signal-to-noise ratio, durability, and long-term usability, which tends to impact the context of rehabilitation and sports medicine.

To begin validation testing, it was essential to implement the hardware designed and conditioned for both EMG and EIT (Figure 11). This system consists of two main modules: Figure 11a, responsible for the acquisition and processing of EMG signals, and Figure 11b, dedicated to EIT measurements.

The EMG module allows for accurate measurement of electrical activity in the biceps, effectively minimizing noise and ensuring signal capture. This capability is essential for assessing muscle function during rehabilitation or clinical evaluations. The EIT module incorporates a 1 mA controlled current injection system with a 16-electrode array, allowing for the reconstruction of tissue impedance images using 104 measurements. This configuration facilitates the analysis of structural and functional changes in tissue, providing valuable information on muscle tissue properties and the effectiveness of rehabilitation treatments.

Furthermore, the integration of both modules allows for a comprehensive assessment of muscle electrical activity and impedance profiles, providing a more comprehensive view of muscle health and performance. However, it is important to note that measurements are not consistent across individuals due to personal variations such as sex, race, and other biological patterns, which constitutes one of the most significant challenges in processing the information. Differences in each person's morphology and physiological characteristics can influence the accuracy of the results, requiring specific adjustments and considerations when interpreting the data. The results of these tests will be critical to validating the system's accuracy and reliability for future clinical and research applications.

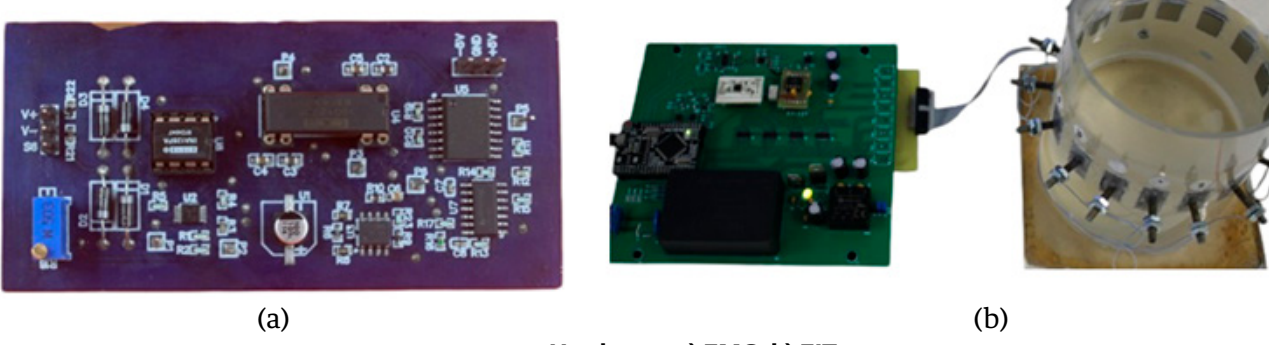


FIGURE 11. Hardware. a) EMG. b) EIT.

To establish a point of comparison, EMG signals recorded with different electrode materials were analyzed and compared with those acquired with Ag/AgCl electrodes, which are widely recognized as the gold standard in medical applications. Figure 12 presents the morphology of the obtained signals, revealing subtle variations between electrode types. Although these differences may seem minimal at first glance, they could introduce bias in subsequent analyses, particularly when advanced signal processing techniques are applied. Therefore, assessing these discrepancies is crucial for selecting electrodes that ensure accuracy and reliability in EMG studies.

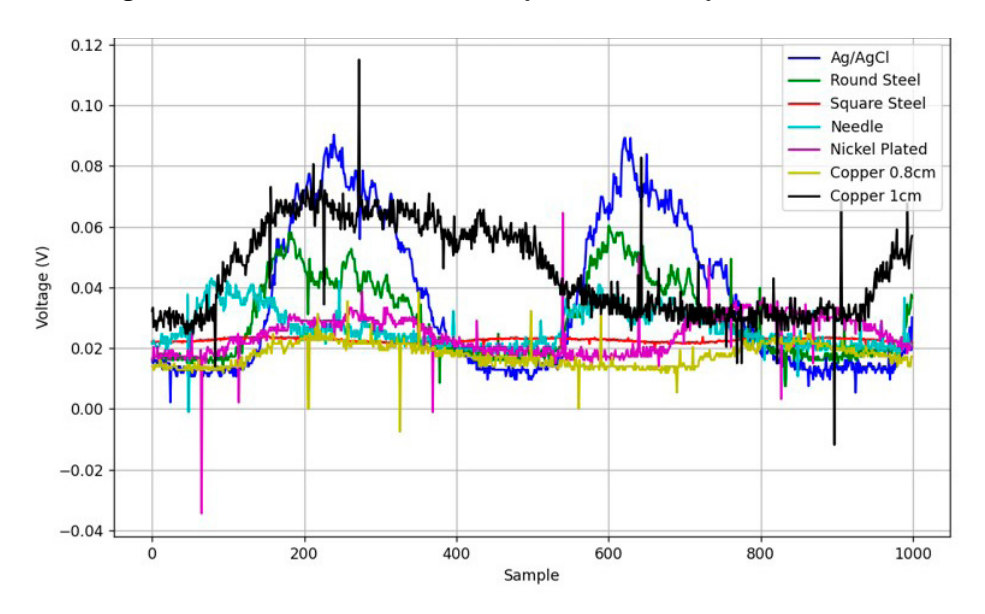


FIGURE 12. EMG signals obtained from the different materials implemented.

To assess the quality and effectiveness of the data obtained, two multivariate regression techniques were applied: principal component regression (PCR) and partial least squares regression (PLSR). These methodologies allowed for in-depth data analysis and the extraction of relevant patterns that facilitated comparisons between the different types of electrodes used. The results obtained from these analyses provided crucial information on the factors affecting the selection of electrodes made of various materials, including stainless steel, copper, nickel, and conventional Ag/AgCl electrodes.

Principal component analysis (PCA) was implemented due to its ability to decompose complex signals into simpler components. This technique allowed for the detailing of the spectral characteristics of the signals in specific time windows, focusing on local maxima that indicate the dominant frequencies in each time segment. This approach is

useful for understanding the dynamic properties of EMG signals, especially during their duration and under different conditions of muscular exertion. The use of PCA facilitated the identification of frequency patterns that are crucial for detecting muscle behavior before and after reaching muscle failure.

Figure 13 illustrates the principal component spectral analysis applied to the five volunteers, using the various electrode materials. This analysis clearly shows the variations in the response of each electrode type as it approaches muscle failure, a critical point for assessing electrode reliability under extreme conditions of use. In particular, the round stainless-steel electrodes and the Ag/AgCl electrodes showed quite similar responses, suggesting that both materials have comparable performance in terms of signal fidelity. However, the stainless-steel electrodes showed greater resistance to noise and hysteresis, meaning they have greater stability in their measurements during the analysis. Furthermore, these stainless-steel electrodes demonstrated a superior ability to tolerate the frequency ranges required for EIT measurements, making them more suitable for such applications.

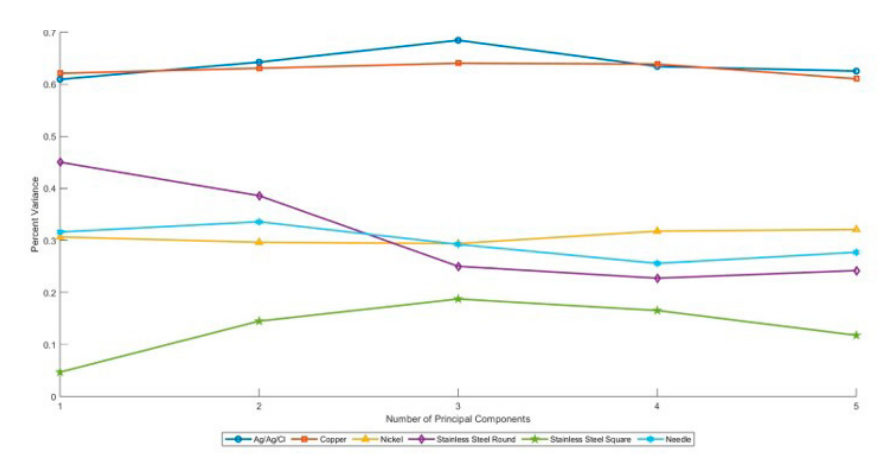


FIGURE 13. Results of Spectral Analysis of Principal Components (PCSA) for Various Electrodes Used in EMG Measurements.

Similarly, the results obtained using partial least squares regression (PLSR) closely matched those found through PCR, as illustrated in Figure 14. This consistency between the two techniques reinforces the reliability of the results and demonstrates the robustness of the methods applied, providing a solid basis for electrode selection and evaluation in future clinical and research applications.

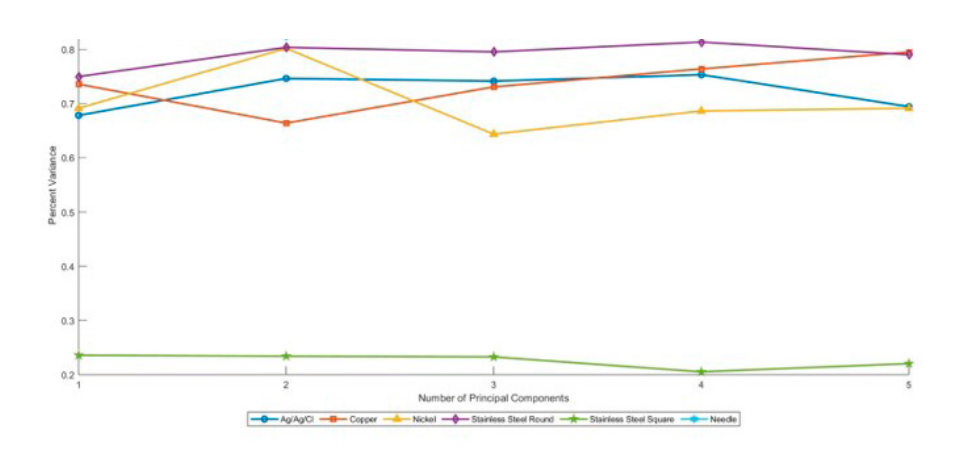


FIGURE 14. Spectral Data Analysis of EMG Using Partial Least Squares Regression (PLSR).

Once the stainless-steel circular electrodes were selected as the optimal option for EMG signal acquisition, measurements were taken on the participants before and after muscle failure during isotonic and isometric contractions. To assess the stability and variability of the recorded signals, statistical metrics such as the mean, standard deviation, and median were analyzed. The mean provided a representative value of muscle activity at each stage of the experiment, while the standard deviation helped quantify signal variability, providing information on the stability of electrical activity over time. Furthermore, the median was used as a robust metric against potential outliers, ensuring a more accurate assessment of the central tendency in the EMG data. These metrics were essential for comparing the effects of muscle exertion on the signal and validating the effectiveness of the selected electrodes under dynamic and static conditions (Figure 15).



FIGURE 15. EMG metrics for the 5 patients.

Continuing with the analysis of electrode materials, the results presented in Table 4 show that stainless steel electrodes, both square and round, exhibit the lowest impedance values when placed over the biceps, with 322  $\Omega$  and 750  $\Omega$ , respectively. These findings suggest that stainless steel electrodes provide more efficient signal acquisition by reducing resistance to current flow and minimizing signal loss. Low impedance is a crucial feature in electrophysiology studies, since high impedance can generate signal distortion, loss of relevant information, and increased electrical noise, which affects the quality of the analysis.

From a practical perspective, lower impedance allows for better transmission of electrical signals from the skin to the acquisition system, favoring a higher signal-to-noise ratio. This is especially relevant in dynamic measurements, where variations in electrode contact pressure can alter signal stability. In this regard, the square stainless-steel electrode, with the lowest recorded impedance (322  $\Omega$ ), demonstrated superior performance, providing more stable measurements and with less susceptibility to signal fluctuations, making it an ideal choice for EMG and EIT applications.

In contrast, copper and nickel alloy electrodes exhibited higher impedance values (greater than 1100  $\Omega$ ), indicating greater electrical resistance at the electrode-skin interface. This behavior translates into lower signal transfer efficiency, which can lead to amplitude attenuation and greater measurement distortion. In applications such as electrical impedance tomography (EIT), where signal quality is critical for image reconstruction accuracy, an increase in impedance can negatively affect spatial resolution and the detection of tissue impedance variations, compromising the clinical interpretation of the results.

Another aspect to consider is the reusability and durability of the materials. Unlike Ag/AgCl electrodes, which, while low impedance, are disposable and require a conductive gel to optimize their performance, stainless steel electrodes offer a more sustainable and cost-effective long-term alternative. Their resistance to corrosion and degradation allows for repeated use without compromising signal quality, making them ideal for long-term studies and applications in research and rehabilitation.

Type Electrode	Impedance
Needle.	1104 Ω
Square Stainless-steel.	322 Ω
Circular Stainless-steel.	750 Ω
Circular electrode (1 cm Ø) with a copper alloy.	1134 Ω
Circular electrode (0.8 cm $\varnothing$ ) with a copper alloy.	1204 Ω
Circular electrode with a nickel alloy.	1120 Ω

**TABLE 4. Impedances for each material** 

Since the square stainless-steel electrodes presented lower impedance, high corrosion resistance, excellent electrical conductivity, and reusability, ex vivo experiments were conducted using a controlled model designed to identify regions with fatty content. In the experiment, a fresh piece of meat containing adipose tissue was carefully prepared to preserve its electrical and structural properties. The adipose tissue was strategically placed between electrodes 1 and 2, as well as between electrodes 4 and 5, as shown in Figure 16. To simulate the dielectric properties of biological tissues, an alternating current of 1 mA at 50 kHz was applied, ensuring conditions representative of real-life clinical applications.

This experimental setup allowed the electrodes to be evaluated for their ability to detect impedance variations associated with fat distribution, providing crucial information on their sensitivity and performance in EIT applications. Furthermore, the study served to validate the durability and efficiency of the stainless-steel electrodes under controlled laboratory conditions prior to their use in in vivo experiments with human subjects.

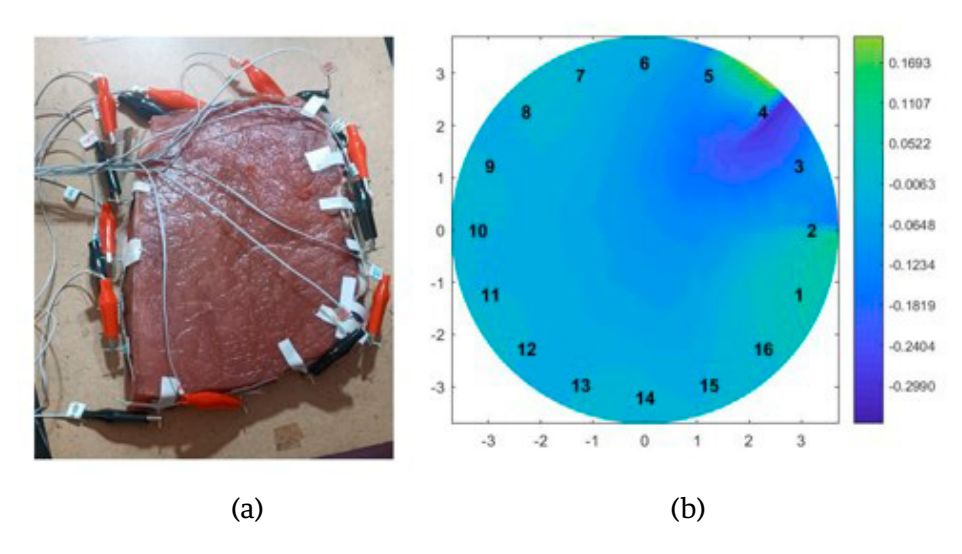


FIGURE 16. Experimental tests with meat. a) Piece of meat. b) Image reconstruction.

Following ex vivo validation experiments, EIT measurements were performed in a group of volunteer subjects to assess impedance variations associated with muscle contractions and fatigue. The objective of these tests was to evaluate real-time changes in muscle conductivity before and after reaching muscle failure, which provided valuable information on physiological responses to exercise.

Each participant underwent a standardized exercise protocol, performing a series of controlled isotonic and isometric contractions targeting the biceps brachii muscle. Isotonic exercises involved dynamic muscle contractions using a dynamometer, while isometric contractions required muscle activation without joint movement, generating varying levels of muscle stress. To ensure consistency, each subject repeated the exercises until reaching muscle failure, defined as the point at which the muscle could no longer generate sufficient force to sustain the contraction.

During the protocol, EIT measurements were performed at predefined time intervals, capturing impedance changes during the different phases of contraction and fatigue. This required applying a current of 1 mA at 50 kHz, which allowed for greater sensitivity.

The results revealed progressive impedance variations correlated with muscular effort and fatigue. Figure 17 shows the reconstructions applied to a subject across the various sessions. Initially, impedance decreased during muscle contractions due to increased intracellular ionic mobility and vascular perfusion, improving tissue conductivity. However, as fatigue set in, the trend reversed, and impedance gradually increased. This change was attributed to localized metabolic accumulation, such as lactic acid buildup and tissue oxygen depletion, which led to alterations in cell membrane properties and a reduction in ionic flux. Furthermore, vasodilation and increased blood accumulation in fatigued muscle contributed to the signal variations, confirming the potential of EIT to detect fatigue-induced physiological changes.

These findings demonstrate the suitability of EIT for real-time muscle assessment, offering a noninvasive and dynamic alternative for monitoring muscle function, endurance, and fatigue progression. This technique holds promise for rehabilitation protocols, allowing clinicians to monitor muscle recovery and optimize treatment strategies for patients undergoing physical therapy or athletic training. Furthermore, the ability to detect subtle changes in conductivity associated with muscle fatigue could pave the way for new applications in sports science, occupational health, and biomedical research.

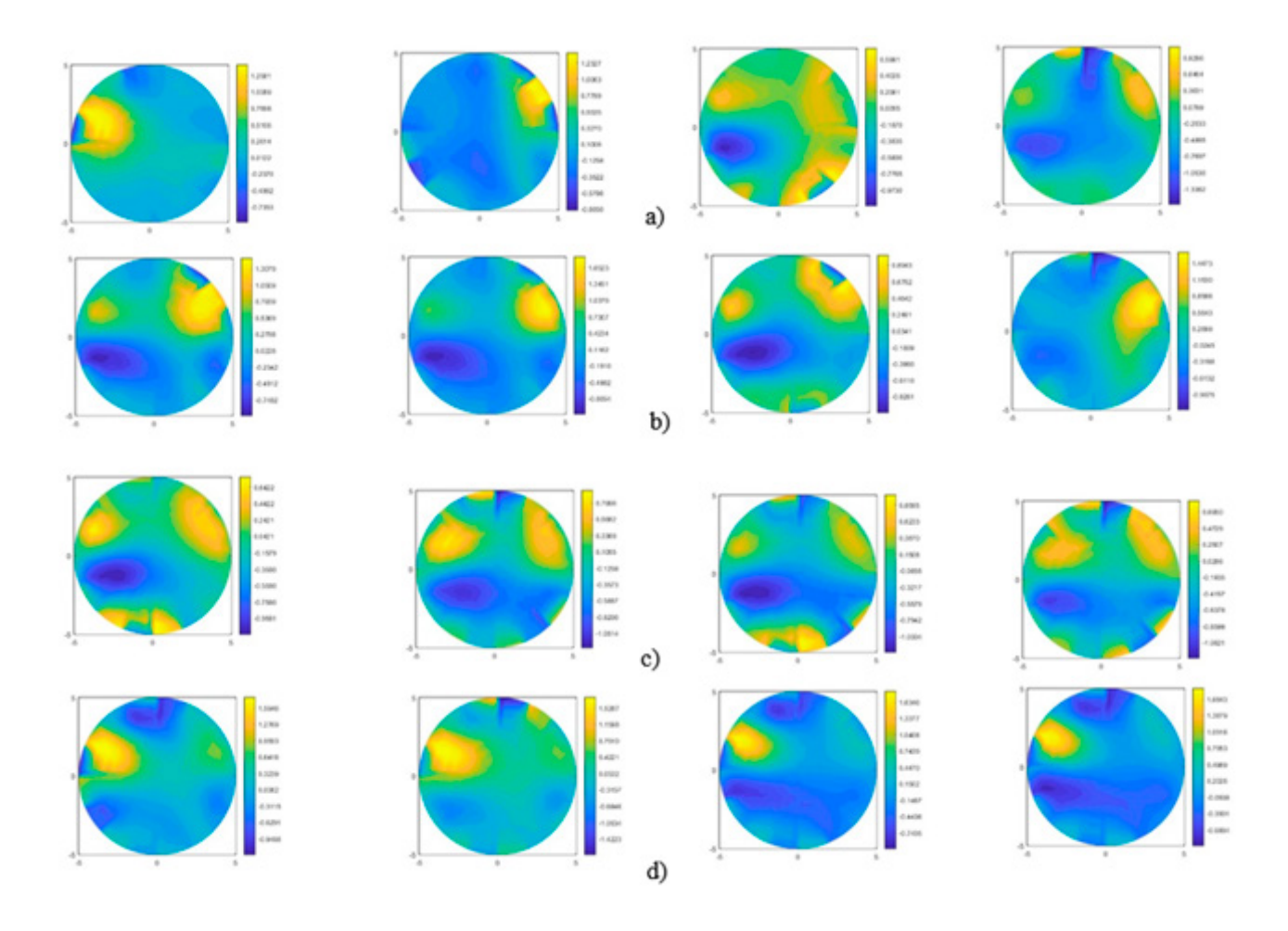


FIGURE 17. Subject 1 EIT reconstructions using Isometric Contraction to Failure, Isotonic Contraction to Failure, Isometric Contraction to Failure, and Isotonic Contraction to Failure. a) Session 1. b) Session 2. c) Session 12. d) Session 13

#### **CONCLUSIONS**

The integration of EMG and EIT has proven to be an effective and complementary strategy for obtaining detailed information on muscle activity, tissue composition, and physiological responses to exercise. This study demonstrates that combining these techniques allows for a more comprehensive assessment of muscle function, capturing both electrical activity and impedance variations, crucial for understanding muscle contraction dynamics, the onset of fatigue, and vascular adaptations.

A key finding of this study is the superior performance of square stainless-steel electrodes, which exhibited the lowest contact impedance (322  $\Omega$ ) among the materials tested. Their high conductivity, stability, and reusability make them the optimal choice for EMG-EIT systems, particularly in rehabilitation settings where accurate and reliable data collection is essential. Compared with alternative materials, these electrodes not only improve signal quality and image reconstruction accuracy but also offer a cost-effective and sustainable alternative to conventional Ag/AgCl electrodes.

Ex vivo and in vivo experiments further validate the practical applicability of this approach, as the results show that EIT can effectively capture muscle impedance variations before and after muscle failure, revealing information about changes in vascularization, metabolic accumulation, and fatigue-induced conductivity changes. This highlights the potential of EIT as a noninvasive tool for assessing muscle function, offering real-time monitoring capabilities that could revolutionize fields such as rehabilitation, sports science, and neuromuscular diagnostics.

#### Limitations

While this study provides valuable information on electrode optimization for EMG and EIT signal acquisition, it has some limitations. First, the study sample was limited to five male participants, which could affect the generalizability of the results to more diverse populations in terms of gender, age, and physiological conditions. Furthermore, although different types of electrodes are compared in terms of efficiency and signal quality, factors such as variability in electrode placement and skin conditions could influence the results. Furthermore, the study focused on signal acquisition under controlled laboratory conditions, which could differ from performance in clinical settings or real-world applications.

#### **Future work**

Future research will focus on improving signal processing techniques, optimizing electrode placement strategies, and refining impedance imaging algorithms to further enhance the resolution and diagnostic capabilities of EMG-EIT systems. Furthermore, expanding studies to include patients with neuromuscular disorders, high-performance athletes, and/or older adults to tailor their use to different clinical needs could lead to personalized rehabilitation protocols and more effective therapeutic interventions. Furthermore, exploring their efficacy under long-term monitoring and dynamic conditions could provide key insights for their application in portable and wearable devices.

#### **ACKNOWLEDGMENT**

The authors wish to express their most sincere gratitude for the scholarship support provided by CONAHCYT.

Furthermore, we wholeheartedly thank the ITMorelia Graduate Department for providing us with essential measurement tools and resources. Their support and collaboration have significantly improved the quality of our work and we deeply appreciate the opportunities they have given us.

#### **DECLARATION OF INTEREST STATEMENT**

The authors report no declaration of interest.

#### CONTRIBUTIONS OF THE AUTHORS

I. A. M. U. conceptualization, methodology, data curation, writing – original draft; J. A. G. G. and A. G. V. software, validation, formal analysis, writing – review & editing; E. R. A., J. C. O. R., A. M. P., and A. I. R. A. investigation, resources, supervision, project administration. All authors have read and approved the final version of the manuscript and agree to its submission to the RMIB proceedings.

#### REFERENCIAS

- [1] E. Criswell, Cram's Introduction to Surface Electromyography, 2nd ed., London, U.K: Jones & Bartlett Learning, 2010.
- [2] R. Merletti and P. J. Parker, Electromyography: Physiology, Engineering, and Non-Invasive Applications, 1st ed., Hoboken, New Jersey, U.S.: John Wiley & Sons, 2005.
- [3] E. A. Clancy and N. Hogan, "Probability density of the surface electromyogram and its relation to amplitude detectors," IEEE Trans. Biomed. Eng., vol. 46, no. 6, pp. 730-739, 1999, doi: https://doi.org/10.1109/10.764949
- [4] D. Yang, et al., "Dynamic training protocol improves the robustness of PR-based myoelectric control," Biomed. Signal Process. Control, vol. 31, pp. 249-256, 2017, doi: https://doi.org/10.1016/j.bspc.2016.08.017
- [5] M. V. Arteaga, et al., "EMG-driven hand model based on the classification of individual finger movements," Biomed. Signal Process. Control, vol. 58, 2020, art. no. 101834, doi: https://doi.org/10.1016/j.bspc.2019.101834
- [6] L. Bi, A. -->Genetu Feleke and C. Guan, "A review on EMG-based motor intention prediction of continuous human upper limb motion for human-robot collaboration," Biomed. Signal Process.Control, vol. 51, pp. 113-127, 2019, doi: https://doi.org/10.1016/j.bspc.2019.02.011
- [7] R. Wen, et al., "Force-Guided High-Precision Grasping Control of Fragile and Deformable Objects Using sEMG-Based Force Prediction," IEEE Robot. Automat. Lett., vol. 5, no. 2, pp. 2762-2769, 2020, doi: https://doi.org/10.1109/lra.2020.2974439
- [8] A. J. Young, L. J. Hargrove and T. A. Kuiken, "The Effects of Electrode Size and Orientation on the Sensitivity of Myoelectric Pattern Recognition Systems to Electrode Shift," IEEE Trans. Biomed. Eng., vol. 58, no. 9, pp. 2537-2544, 2011, doi: https://doi.org/10.1109/tbme.2011.2159216
- [9] L. Hargrove, K. Englehart and B. Hudgins, "A training strategy to reduce classification degradation due to electrode displacements in pattern recognition based myoelectric control," Biomed. Signal Process. Control, vol. 3, no. 2, pp. 175-180, 2008, doi: https://doi.org/10.1016/j.bspc.2007.11.005
- [10] Y. Geng, P. Zhou and G. Li, "Toward attenuating the impact of arm positions on electromyography pattern-recognition based motion classification in transradial amputees," J. NeuroEng. Rehabil., vol. 9, no. 1, 2012, art. no. 74, doi: https://doi.org/10.1186/1743-0003-9-74
- [11] A. Fougner, et al., "Resolving the Limb Position Effect in Myoelectric Pattern Recognition," IEEE Trans. Neural Syst. Rehabil. Eng., vol. 19, no. 6, pp. 644-651, 2011, doi: https://doi.org/10.1109/tnsre.2011.2163529
- [12] D. Tkach, H. Huang and T. A. Kuiken, "Study of stability of time-domain features for electromyographic pattern recognition", J. NeuroEng. Rehabil., vol. 7, 2010, art. no. 21, doi: https://doi.org/10.1186/1743-0003-7-21
- [13] J. W. Sensinger, B. A. Lock and T. A. Kuiken, "Adaptive Pattern Recognition of Myoelectric Signals: Exploration of Conceptual Framework and Practical Algorithms", IEEE Trans. Neural Syst. Rehabil. Eng., vol. 17, no. 3, pp. 270-278, 2009, doi: https://doi.org/10.1109/tnsre.2009.2023282
- [14] Q. Xi, et al., "A novel localized collocation solver based on Trefftz basis for potential-based inverse electromyography", Appl. Math. Computation, vol. 390, 2021, art. no. 125604, doi: https://doi.org/10.1016/j.amc.2020.125604
- [15] K. van den Doel, U. M. Ascher and D. K. Pai, "Source localization in electromyography using the inverse potential problem", Inverse Probl., vol. 27, no. 2, 2011, art. no. 025008, doi: https://doi.org/10.1088/0266-5611/27/2/025008
- [16] P. S. Cuculich, et al., "Noninvasive real-time mapping of an incomplete pulmonary vein isolation using electrocardiographic imaging", Heart Rhythm, vol. 7, no. 9, pp. 1316-1317, 2010, doi: https://doi.org/10.1016/j.hrthm.2009.11.009
- [17] P. S. Cuculich et al., "The Electrophysiological Cardiac Ventricular Substrate in Patients After Myocardial Infarction," J. Amer. College Cardiol., vol. 58, no. 18, pp. 1893-1902, 2011, doi: https://doi.org/10.1016/j.jacc.2011.07.029
- [18] J. Sun, et al., "Application of Surface Electromyography in Exercise Fatigue: A Review," Frontiers Syst. Neurosci., vol. 16, Agu. 2022, Art. no. 893275, doi: https://doi.org/10.3389/fnsys.2022.893275
- [19] A. J. Young, L. J. Hargrove and T. A. Kuiken, "The Effects of Electrode Size and Orientation on the Sensitivity of Myoelectric Pattern Recognition Systems to Electrode Shift,", IEEE Trans. Biomed. Eng., vol. 58, no. 9, pp. 2537-2544, 2011, doi: https://doi.org/10.1109/tbme.2011.2159216
- [20] I. Morgado, Materia gris: La apasionante historia del conocimiento del cerebro, Spain: Ariel, 2021.
- [21] M. Garzón Barrios, et al., "El efecto volta. Un caso de estudio sobre la producción de efectos sensibles y los procesos de teorización en ciencias," Ens. Pesqui. Em Educ. Em Cienc. (Belo Horizonte), vol. 22, 2020, art. no. e14862, doi: https://doi.org/10.1590/1983-21172020210113

- L. K. Huang, et al., "Electrical Impedance Myography Applied to Monitoring of Muscle Fatigue During Dynamic Contractions," IEEE Access, vol. 8, pp. 13056-13065, 2020, doi: https://doi.org/10.1109/access.2020.2965982
- [23] H. F. Hassan, S. J. Abou-Loukh and I. K. Ibraheem, "Teleoperated robotic arm movement using electromyography signal with wearable Myo armband," J. King Saud Univ. Eng. Sci., vol. 32, no. 6, pp. 378-387, 2020, doi: https://doi.org/10.1016/j.jksues.2019.05.001
- [24] J. N. Wang et al., "Optimization of the electrode configuration of electrical impedance myography for wearable application," Automatika, vol. 61, no. 3, pp. 475-481, 2020, doi: https://doi.org/10.1080/00051144.2020.1783615
- [25] T. J. Freeborn, G. Regard and B. Fu, "Localized Bicep Tissue Bioimpedance Alterations Following Eccentric Exercise in Healthy Young Adults," IEEE Access, vol. 8, pp. 23100-23109, 2020, doi: https://doi.org/10.1109/access.2020.2970314
- [26] T. Freeborn and B. Fu, "Fatigue-Induced Cole Electrical Impedance Model Changes of Biceps Tissue Bioimpedance," Fractal Fract., vol. 2, no. 4, 2018, art. no. 27, doi: https://doi.org/10.3390/fractalfract2040027
- [27] S. B. Rutkove and B. Sanchez, "Electrical Impedance Methods in Neuromuscular Assessment: An Overview," Cold Spring Harb. Perspect. Med., vol. 9, no. 10, 2018, art. no. a034405, doi: https://doi.org/10.1101/cshperspect.a034405
- [28] R. Merletti, et al., "Advances in Surface EMG: Recent Progress in Detection and Processing Techniques," Crit. Rev. Biomed. Eng., vol. 38, no. 4, pp. 305-345, 2010, doi: https://doi.org/10.1615/critreybiomedeng.v38.i4.10
- [29] M. Rinaldi et al., "Increased lower limb muscle coactivation reduces gait performance and increases metabolic cost in patients with hereditary spastic paraparesis," Clin. Biomechanics, vol. 48, pp. 63-72, 2017, doi: https://doi.org/10.1615/critrevbiomedengw38.i4.10
- [30] M. C. Neves Rosa, et al., "Methodologies to assess muscle co-contraction during gait in people with neurological impairment A systematic literature review," J. Electromyogr. Kinesiol., vol. 24, no. 2, pp. 179-191, 2014, doi: https://doi.org/10.1016/j.jelekin.2013.11.003
- [31] A. Tatarelli et al., "Global Muscle Coactivation of the Sound Limb in Gait of People with Transfemoral and Transtibial Amputation," Sensors, vol. 20, no. 9, 2020, art. no. 2543, doi: https://doi.org/10.3390/s20092543
- [32] D. Farina and R. Merletti, "A novel approach for estimating muscle fiber conduction velocity by spatial and temporal filtering of surface emg signals," IEEE Trans. Biomed. Eng., vol. 50, no. 12, pp. 1340-1351, 2003, doi: https://doi.org/10.1109/tbme.2003.819847
- [33] D. F. Stegeman and H. J. Hermens, "Standards for surface electromyography: The European project Surface EMG for non-invasive assessment of muscles (SENIAM)," Roessingh Res. Develop., vol. 10, pp. 108-112, 2007. [Online]. Avaible: https://www.researchgate.net/profile/Hermie-Hermens/publication/228486725\_Standards\_for\_surface\_electromyography\_The\_European\_project\_Surface\_EMG\_for\_non-invasive\_assessment\_of\_muscles\_SENIAM/links/09e-41508ec1dbd8a6d000000/Standards-for-surface-electromyography-The-European-project-Surface-EMG-for-non-invasive-assessment-of-muscles-SENIAM.pdf
- [34] M. del Olmo Reíllo, "Procesado de señales electromiográficas para la evaluación del esfuerzo muscular en el ámbito deportivo," Trabajo Fin de Grado, Ingeniería Audiovisual y Comunicaciones, Escuela Técnica Superior de Ingeniería y Sistemas de Telecomunicación, Madrid, 2021. [Online]. Available: https://oa.upm.es/69422/1/TFG\_MALENA\_DEL\_OLMO\_REILLO.pdf
- [35] S.-Y. Lee, C.-P. Wang and Y.-S. Chu, "Low-Voltage OTA-C Filter With an Area- and Power-Efficient OTA for Biosignal Sensor Applications," IEEE Trans. Biomed. Circuits Syst., vol. 13, no. 1, pp. 56-67, 2019, doi: https://doi.org/10.1109/tbcas.2018.2882521
- [36] A. Adler and D. Holder, Electrical Impedance Tomography, 2a ed., Boca Raton, Florida, U.S.: CRC Press, 2021, doi:https://doi.org/10.1201/9780429399886
- [37] J. A. Gutierrez-Gnecchi, "Dynamic Link Library and Signal Conditioning System for Electrical Impedance Tomography Virtual Instrumentation," in 2010 IEEE Electron. Robot. and Automotive Mechanics Conf., Cuernavaca, Mexico, Sep. 28-Oct. 1, 2010, pp. 648-653, doi: https://doi.org/10.1109/CERMA.2010.128
- [38] S. Feliu, J. C. Galván and M. Morcillo, "An interpretation of electrical impedance diagrams for painted galvanized steel," Prog. Organic Coatings, vol. 17, no. 2, pp. 143-153, 1989. doi: https://doi.org/10.1016/0033-0655(89)80020-2
- [39] K. A. Dines and R. J. Lytle, "Analysis of electrical conductivity imaging," GEOPHYSICS, vol. 46, no. 7, pp. 1025-1036, 1981, doi: https://doi.org/10.1190/1.1441240
- [40] C.C. Barber, B.H. Brown, and I.L. Freeston, "Imaging spatial distributions of resistivity using applied potential tomography," Electron. Lett., vol. 19, no. 22, pp. 933-935, 1983, doi: https://doi.org/10.1049/el;19830637
- [41] H. C. Jongschaap, et al., "Electrical impedance tomography: a review of current literature," Eur. J. Radiol., vol. 18, no. 3, pp. 165-174, 1994, doi: https://doi.org/10.1016/0720-048x(94)90329-8
- [42] R. Kusche and M. Ryschka, "Combining Bioimpedance and EMG Measurements for Reliable Muscle Contraction Detection," IEEE Sensors J., vol. 19, no. 23, pp. 11687-11696, 2019, doi: https://doi.org/10.1109/jsen.2019.2936171
- [43] H. Nahrstaedt, et al., "Bioimpedance- and EMG-Triggered FES for Improved Protection of the Airway During Swallowing," Biomed. Tech., 2013, doi: https://doi.org/10.1515/bmt-2013-4025
- [44] A. N. Briko, A. V. Kobelev, and S. I. Shchukin, "Electrodes interchangeability during electromyogram and bioimpedance joint recording," in 2018 Ural Symposium on Biomedical Engineering, Radioelectronics and Information Technology, Yekaterinburg, Russia, May 7-8, 2018, pp. 17-20, doi: https://doi.org/10.1109/USBEREIT.2018.8384539
- [45] SENIAM. (n.d.). "Recommendations for sensor locations in arm or hand muscles". [Online]. Available: http://seniam.org/sensor\_location.htm
- [46] J. A. Gutierrez-Gnecchi, et al., "EITQUALITYFOR464X86 [Software]," INDAUTOR 03-2024-072512544400-01, 2024